

Intermittency in a turbulent low temperature gaseous helium jet

 O. Chanal, B. Chabaud, B. Castaing^a, and B. Hébral

Centre de Recherches sur les Très Basses Températures, CNRS, BP 166, 38042 Grenoble Cedex 9, France

Received 13 October 1999 and Received in final form 19 May 2000

Abstract. We analyse experimental velocity measurements on the axis of a low temperature gaseous helium jet. From independent increments arguments, we reproduce the behaviour of structure functions. We show where this approach fails and how the intermittency phenomenon is a small correction. The physical arguments under the multiplicative cascade models for this intermittency imply an acceleration of this cascade close to the dissipative range, which we are able to evidence. This acceleration could be responsible of the apparent Extended Self Similarity between structure functions of various orders.

PACS. 47.27.Wg Jets – 47.27.Gs Isotropic turbulence; homogeneous turbulence – 47.27.Jv High-Reynolds-number turbulence – 05.10.Gg Stochastic analysis methods (Fokker-Planck, Langevin, etc.)

1 Introduction

Intermittency is a striking feature of turbulent flows [1]. It can also be observed in fields as different as the change ratio of money [2,3] or the brightness intensities in pictures [4]. In turbulent flows, it can be defined [5] as the progressive change of shape of the probability density functions of velocity differences at distance r , when r goes from the correlation (integral) length L of the flow, down to the dissipative length η , where the velocity difference is simply proportional to the velocity gradient.

Theoretical discussions of this phenomenon have long been centered on the infinite Reynolds number limit [6]. But the obvious interest of finite Reynolds, and the difficulty to safely extrapolate the experimental results to the infinite limit, led recently to consider the corrections to this limit [7,8]. The question then seriously arose if the viscosity (the Reynolds number) could influence the whole range of scales, from η up to the integral scale L [9–11]. For instance the structure functions of order p : $S_p(r) = \langle |\delta v|^p \rangle$ where δv is the longitudinal velocity difference, or their equivalent based on a more sophisticated wavelet decomposition [11], could be interpreted as a universal function of r^β where β is a Reynolds dependent exponent going to zero when Re goes to infinity [7]. In a parallel but partly related way, these structure functions behave as power laws of each other down to scales obviously influenced by viscosity (Extended Self Similarity or ESS) [12]. This suggests that the same process drives the evolution of the statistics down to these scales [8].

In this paper, in order to lie the discussion on firm basis, we shall try to reproduce the behaviour of the struc-

ture function $S_p(r)$ starting from the most naive arguments of independent increments. We shall see how it fails and how a tiny correction the intermittency phenomenon is. Then we shall track the physical basis lying under the multiplicative process formalism. This will lead us to an equation modelizing the behaviour of structure functions. According to this equation, both the r^β ansatz and ESS are approximations, good at moderate Reynolds numbers, but increasingly bad at higher Reynolds.

2 Experiments

The data we use in this paper are velocity measurements on the axis of a jet, the working fluid being low temperature gaseous helium [13]. The cryogenic hot wire probe is made of AuGe sputtered on a fiber glass, 1.5 μm in diameter [14]. The AuGe layer is 3000 \AA thick and is shortened by a Au+Ag layer, except on a short (0.5 μm) length, which acts as the hot point (Fig. 1). Its resistance is $R = 200 \Omega$ at the working point ($\simeq 15 \text{ K}$ with a gas temperature of 4.3 K). The sensor temperature sensitivity is $|(T/R)dR/dT| \approx 0.45$. It is operated at constant temperature through a homemade anemometer electronics adapted to low temperatures: the balance of a 10 MHz bridge is synchronously detected, low pass filtered (1 MHz), integrated and injected in the probe as a “dc” current. Joule heating, both from the 10 MHz probing current and from the “dc” component, allows to lock the wire temperature at a constant value. The “dc” component is a measurement of the fluid velocity. We shall describe the calibration procedure after the geometry of the jet.

After filtering and laminarizing, He gas goes through a convergent cone, 30° half angle, ending on a nozzle 2 mm in diameter. The jet then develops downwards in a cylindrical chamber of vertical axis, 12 cm in diameter (Fig. 2).

^a Present address: ENSL, 46 allée d’Italie, 69364 Lyon Cedex 07, France

e-mail: bcastain@ens-lyon.fr

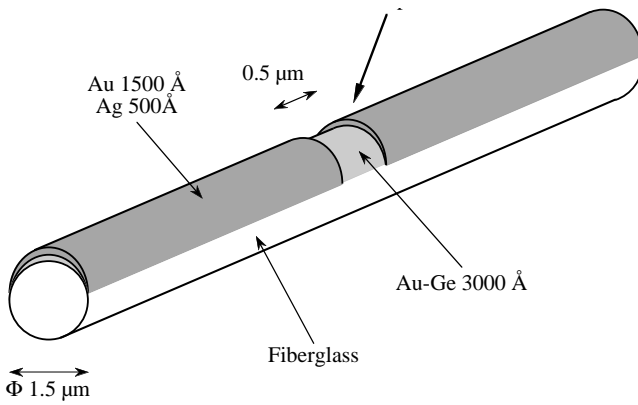


Fig. 1. Scheme of the sensitive part of the sensor.

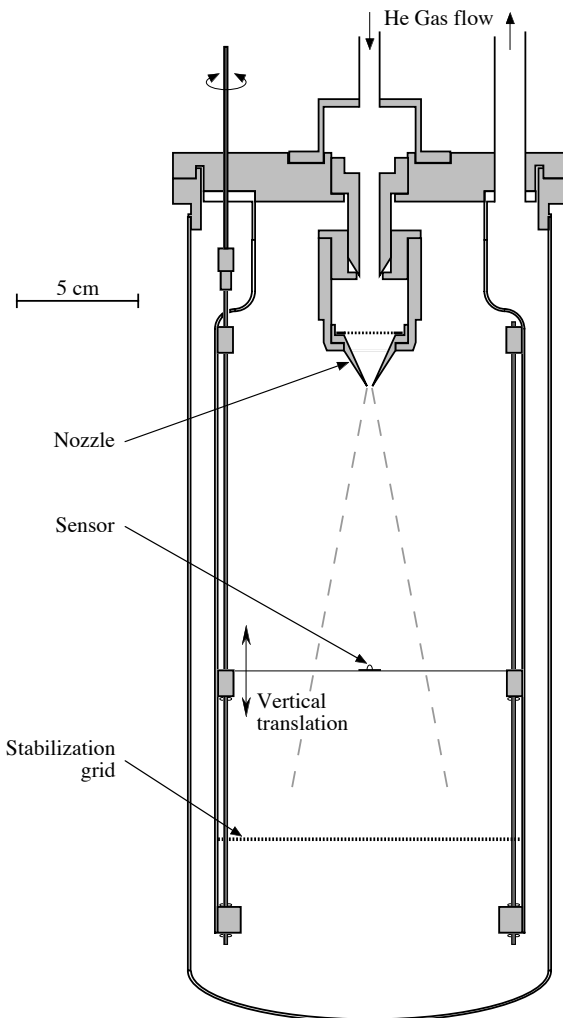


Fig. 2. The experimental cell.

A grid, 16 cm away from the nozzle, stabilizes the jet by breaking the largest eddies before they can interact with the walls. Helium then flows out of the cryostat to a recuperation tank.

The working position of the probe is on the axis, 8 cm away from the nozzle (*i.e.* 40 nozzle diameters). For calibration, we can move the sensor up *in situ* into the nozzle potential cone, but we had troubles with this procedure

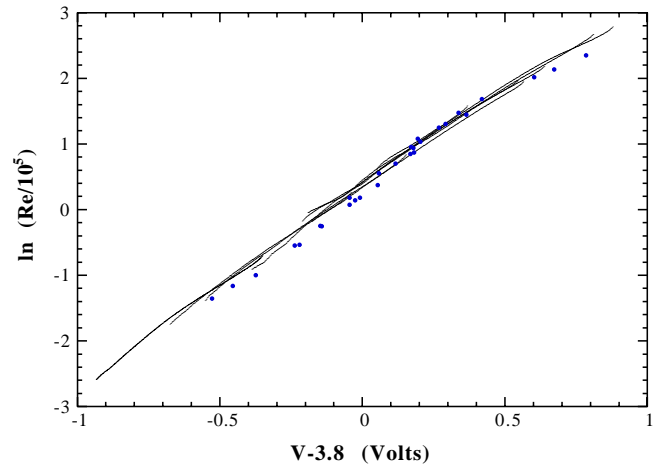


Fig. 3. Experimental sensor calibration points (Reynolds *vs.* voltage) and calibration curves for different Re numbers.

due to bad electrical contacts in the moving connecting wires. We thus positioned the probe at a 8 cm working distance, and we recorded the average signal *versus* the nozzle Reynolds number. We obtained a rough calibration which was mainly used as a verification of the procedure we present now.

Indeed, several studies [15] have shown that the distribution of velocities is nearly Gaussian in turbulent flows, and especially in jets on their axis. Reported discrepancies are close to experimental uncertainties. If we consider this distribution $P(v)$ as known, we can infer the calibration from the observed distribution of the signal s . Let us consider the distribution:

$$P(v) \propto v^2 \exp -\frac{(v - V)^2}{2\tau^2 V^2},$$

where V is experimentally determined from the nozzle Reynolds number and from the distance between the nozzle and the sensor: V is close to the average velocity. The prefactor v^2 takes into account both the sensitivity of our wire to all the velocity components [16] and its inadequacy in the neighbourhood of $v = 0$. τ is the turbulence ratio: taking it as $\tau = 0.23$ gives a nice coincidence between the calibrations based on the various runs, at different Reynolds numbers, and with the previous rough calibration. In Figure 3, we show the comparison. Note the units chosen for the velocity: for direct comparison with the rough calibration above, we express it as the nozzle Reynolds number Re which would result in an average velocity equal to the velocity we measure. Once the calibration relation determined, each measured voltage gives us a number Re related to the instantaneous velocity v through:

$$v = \langle v \rangle Re / \langle Re \rangle,$$

where $\langle Re \rangle$ is the nozzle Reynolds number of the experiment, and $\langle v \rangle$ the average velocity on the probe [14]. In Figure 3, the curves correspond to the calibrations obtained from each experiment through the Gaussian

distribution hypothesis as explained above. The points correspond to the nozzle Reynolds number *versus* the average voltage.

Let us call $c(v)$ (resp. $c'(s)$) the proportion of the data giving a velocity (resp. signal) lower than v (resp. s), *i.e.* we have:

$$\int_{-\infty}^v P(v') dv' = c(v),$$

or

$$P(v) = \frac{dc(v)}{dv}.$$

The calibration $v(s)$ is then obtained from the equality:

$$c(v(s)) = c'(s).$$

As said above, all our measurements are made with a single probe. To obtain longitudinal velocity differences, we refer to the Taylor frozen turbulence hypothesis [1]. However, in a jet, large relative variations of the velocity occur. Using the average flow velocity to convert time in distances is spurious. We rather use the instantaneous velocity in the following way [17]. From a given starting point, we calculate the distances R_i by summing the observed velocities:

$$R_i = \sum_{j < i} v_j \Delta t,$$

where $(\Delta t)^{-1}$ is the sampling frequency. We then determine velocities at regularly spaced points, whose distance is $m \delta x$, by interpolation between v_i and v_{i+1} , where i is such that:

$$R_i < m \delta x \leq R_{i+1}.$$

Those velocities are then taken to reconstruct the regularly spaced velocity file. Figure 4 shows the spectra of the original “temporal” file together with that of the “spatial” file, for one of our runs. The correction has been shown to be equivalent to the Lumley correction for spectra [18].

Let us now say a few words about noise. As the noise is *a priori* uncorrelated with the physical signal, we can correct statistical quantities, such as structure functions, from it. If the noise b can be considered as small compared to the velocity difference, then:

$$\langle (\delta v + \delta b)^p \rangle \approx \langle (\delta v)^p \rangle + \frac{p(p-1)}{2} \langle (\delta b)^2 \rangle \langle (\delta v)^{p-2} \rangle,$$

as $\langle \delta b \rangle = 0$, where $\delta b = b(R+r) - b(R)$ and $\langle \rangle$ stands for ensemble average.

Non integer p are possible only using absolute value moments. Then a formula such as

$$\langle |\delta v|^p \rangle \approx \langle |\delta v + \delta b|^p \rangle - \frac{p(p-1)}{2} \langle (\delta b)^2 \rangle \langle |\delta v + \delta b|^{p-2} \rangle, \quad (1)$$

is rigorously valid only for even integer p , but gives an interpolation formula for all p values.

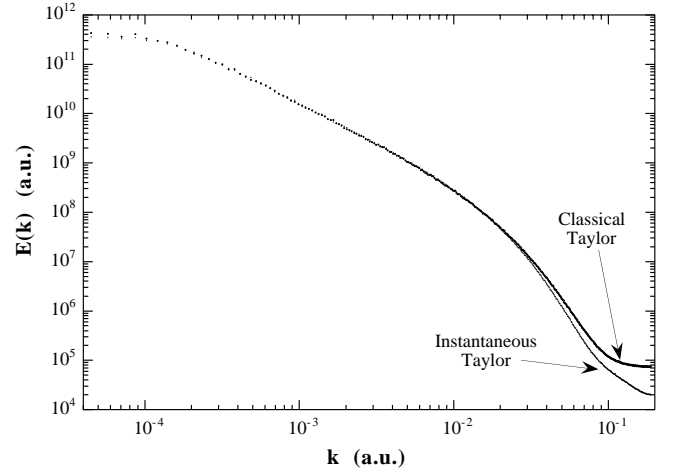


Fig. 4. Comparison between the original temporal spectra and the “reconstructed” spatial one (instantaneous velocity).

Now the noise can be recorded independently as a signal noise n , not directly related to the velocity noise b . If $v(s)$ is our calibration function we can approximate:

$$v(s+n) \approx v(s) + n \frac{dv}{ds} = v(s) + b.$$

Thus, using the noise record and our velocity file, we can construct for each point a model noise:

$$b = n \frac{dv}{ds},$$

whose statistical characteristics, in particular the second moment of differences

$$\langle \delta b^2 \rangle(r),$$

should be identical to those of the real noise which affects our file. Let us stress again that we correct the structure functions, through equation (1), and not the instantaneous velocity (which is impossible). Figure 5 shows the logarithmic derivative of the third structure function with and without the correction. While the uncorrected one is affected by the noise at rather large r , the corrected one goes at higher values, closer to 3, at small distance r .

3 Kolmogorov 41 and velocity diffusion

Figure 6 gives the logarithmic derivative of $\langle |\delta v|^3 \rangle(r)$ for various Taylor scale based Reynolds numbers R_λ [1]. The abscissa are slightly shifted by a factor (20% correction at most without any trend *versus* R_λ) to make the data coinciding at the point where they go to zero, in order to stress the identity of their variations at large r . Indeed the figure can be interpreted by the observation that the behaviours are apparently independent of the Reynolds number down to the point where dissipation occurs.

This observation is the very basis of Kolmogorov 41 analysis, except that in this frame the non-dissipative

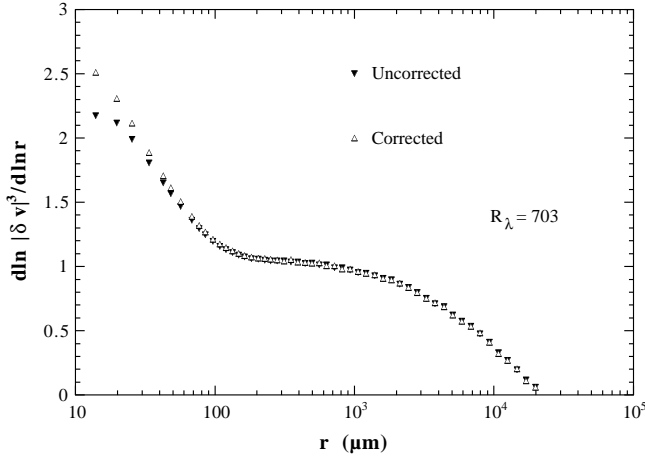


Fig. 5. Logarithmic derivative of the third structure function with and without noise correction.

range is generally modeled by a power law-behaviour for $\langle |\delta v|^p \rangle$ *i.e.* a plateau for the logarithmic derivative. Clearly, limiting oneself to a plateau region would strongly reduce the interesting range, and even cancel it as the influence of large scale goes far down. The importance of addressing the finite Reynolds problem has been central in the last decade research on turbulence (see [5, 7–13, 19, 20] but also the recent work [21–23]). Here we need a Kolmogorov 41 model for finite Reynolds. It can be obtained remarking that it corresponds in its spirit to a diffusion in the velocity space, the diffusion constant being ϵ , the dissipated power per unit mass.

The saturation of $\langle |\delta v|^p \rangle$ at large scales is then reminiscent of the physics of the Langevin model for Brownian motion, where the friction term saturates the r.m.s. velocity at large times. Let us write a Langevin equation for the velocity difference between two points [24]:

$$\dot{\delta v} = -\gamma \delta v + f(t), \quad (2)$$

where $f(t)$ is a δ correlated noise:

$$\langle f(t_1)f(t_2) \rangle = \epsilon \delta(t_1 - t_2). \quad (3)$$

The Langevin equation integrates in:

$$\delta v(t) = \int_0^t e^{-\gamma(t-t')} f(t') dt',$$

which gives for the second moment:

$$\begin{aligned} \langle \delta v^2 \rangle &= \frac{\epsilon}{2\gamma} (1 - e^{-2\gamma t}) \\ &= v_0^2 E(\gamma t). \end{aligned} \quad (4)$$

Integrating again gives for the distance:

$$r(t) = \int_0^t dt' \int_0^{t'} e^{-\gamma(t'-t'')} f(t'') dt'',$$

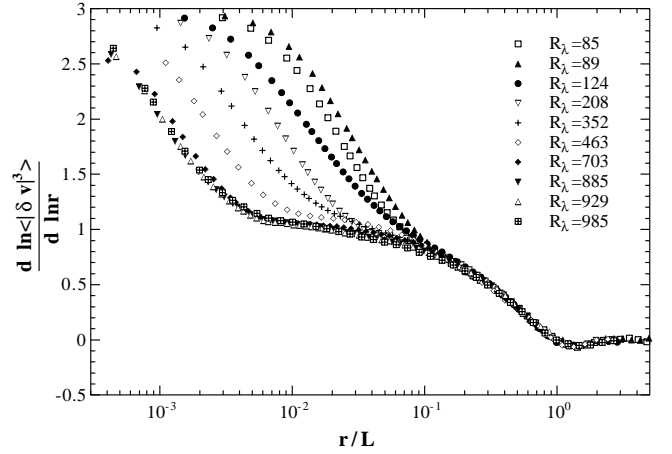


Fig. 6. Logarithmic derivative of $\langle |\delta v|^3 \rangle$ vs. r for various Taylor scale based Reynolds numbers.

and for the mean squared distance:

$$\begin{aligned} \langle r^2 \rangle &= \frac{\epsilon}{\gamma^3} \left\{ 2(\gamma t + e^{-\gamma t} - 1) - (1 - e^{-\gamma t})^2 \right\} \\ &= \frac{\epsilon}{\gamma^3} F(\gamma t). \end{aligned} \quad (5)$$

For small γt , we obtain:

$$\langle \delta v^2 \rangle = \epsilon t; \quad \langle r^2 \rangle = \frac{2}{3} \epsilon t^3. \quad (6)$$

The second formula is the Richardson law [25]. Assimilating $\langle r^2 \rangle$ with the square of the distance gives $\langle \delta v^2 \rangle = ((3/2)\epsilon^2 r^2)^{1/3}$.

On the other hand, the large scale saturation gives γ being proportional to ϵ :

$$\gamma = \frac{\epsilon}{2v_0^2}. \quad (7)$$

The physical interpretation is that the large scale velocity differences amplitude results from the competition between two effects: a random, δ correlated noise which tends to make it grow, and a damping γ which limits the memory of this noise to a typical time $1/\gamma$.

We now have a model for infinite Reynolds but no dissipative transition. Indeed what physically occurs in the small scales $r < \eta$, where η is a dissipative scale, is that velocity differences are proportional to r , that is f is proportional to r . This can be taken into account, in an *ad hoc* (*i.e.* approximate) way corresponding to the famous Batchelor ansatz, replacing in equations (4, 5) ϵ by:

$$\epsilon' = \epsilon \frac{r^2}{r^2 + \eta^2}. \quad (8)$$

Then:

$$r^2 = \frac{\epsilon}{\gamma^3} \frac{r^2}{r^2 + \eta^2} F(\gamma t), \quad (9)$$

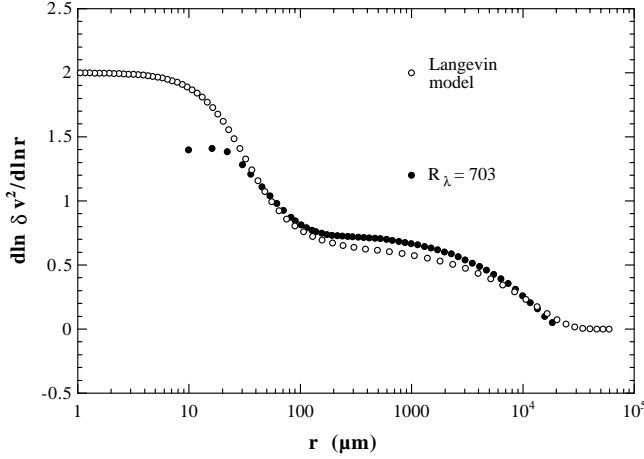


Fig. 7. Experimental results for the logarithmic derivative of $\langle \delta v^2 \rangle$, compared with the Langevin model.

and

$$r^2 + \eta^2 = \frac{\epsilon}{\gamma^3} F(\gamma t), \quad (10)$$

which gives γt and thus

$$\langle \delta v^2 \rangle = \frac{r^2 v_0^2}{r^2 + \eta^2} E(\gamma t). \quad (11)$$

Figure 7 compares the experimental results for the logarithmic derivative of $\langle \delta v^2 \rangle$ with this model where the only adjustable parameter is η , *i.e.* the Reynolds number.

4 Intermittency

The fact that the Kolmogorov 41 theory (K 41) gives an overall good account of the behaviour of low order structure functions is indeed well known. However, the progressive change in shape of the probability distribution function (pdf) of δv with r is generally seen as a proof of the inadequacy of K 41 and is referred to as the phenomenon of intermittency. If the various moments of δv only depend on ϵ and r , then

$$u = \frac{\delta v}{(\epsilon r)^{1/3}},$$

must have a universal distribution. But this is in fact an infinite Reynolds number argument. It not only assumes independence *versus* v_0 and η . It also assumes independence *versus* the distribution of $f(t)$. If f is not Gaussian, then the fourth cumulant of δv will be non-zero and proportional to t in the Langevin model of the previous section, for small enough t :

$$\langle \delta v^4 \rangle - 3\langle \delta v^2 \rangle^2 = a_4 t.$$

In the same limit $\langle \delta v^2 \rangle = \epsilon t$, and:

$$\frac{\langle \delta v^4 \rangle}{\langle \delta v^2 \rangle} = 3\langle \delta v^2 \rangle + \frac{a_4}{\epsilon}.$$

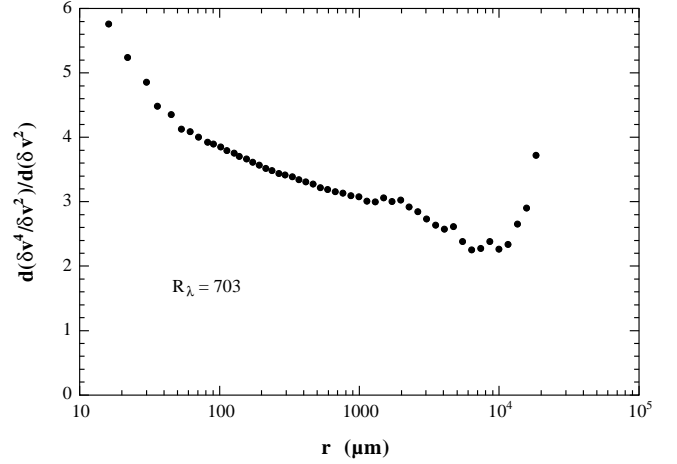


Fig. 8. Derivative of $\langle \delta v^4 \rangle / \langle \delta v^2 \rangle$ versus $\langle \delta v^2 \rangle$.

Thus the derivative of this ratio *versus* $\langle \delta v^2 \rangle$ should be constant, equal to 3. This is plotted in Figure 8. Although tiny, the discrepancy is clear. An independent increments model, as the Langevin model of the previous section, cannot account for this discrepancy. The memory it implies is generally attributed to the inhomogeneity of the dissipation ϵ , which would make, in the Langevin model, the diffusion coefficient to vary. It can be described by a multiplicative cascade.

5 Physical soundness of the cascade

It must be emphasized, from the beginning, that the multiplicative cascade approach is completely different from the previous, velocity diffusion, one. The only compatibility between the two approaches raises unsolved problems which go outside the scope of this paper. We simply remark that, as for the diffusion one, this multiplicative approach has some success in describing turbulent flows. It seems thus worthwhile to follow and to test its logic.

The multiplicative approach lies on the assumption that universal relations exist between the δv pdfs at different scales (we shall limit ourself to the absolute values $\langle |\delta v| \rangle$):

$$P_r(|\delta v|) = \int G_{rr'}(\ln \alpha) \frac{1}{\alpha} P_{r'}\left(\frac{|\delta v|}{\alpha}\right) d \ln \alpha, \quad (12)$$

with $r < r'$ [8, 18, 19].

Such a relation can be interpreted in two different ways. Velocity differences at scale r appear as those at scale r' multiplied by a random factor α , the logarithm of which having the distribution $G_{rr'}$. In the spirit of the Kolmogorov-Obukov 62 theory (KO 62) typical velocities at scale r go like $(\epsilon_r r)^{1/3}$. Thus:

$$\alpha = \left(\frac{\epsilon_r}{\epsilon_{r'}} \frac{r}{r'} \right)^{1/3}, \quad (13)$$

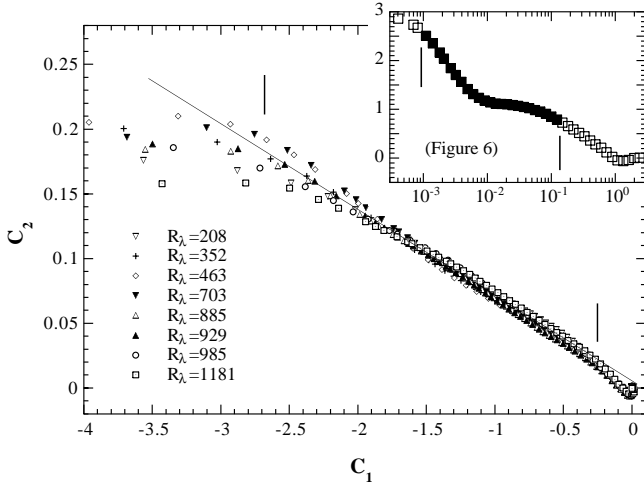


Fig. 9. Behaviour of C_2 versus C_1 for different Reynolds numbers.

and the distribution of α comes from the distribution of the local ratios $\epsilon_r/\epsilon_{r'}$, where ϵ_r is the local energy transfer rate at scale r .

This is the physical interpretation which relates the multiplicative velocity cascade to the energy cascade down the scales, toward dissipation. On a formal point of view, one can remark that the above relation is a convolution when expressed in the $\ln|\delta v|$ variable. This is due to the translation symmetry in $\ln|\delta v|$. Multiplying all the velocities of the flow by the same factor does not change anything to the physics if we simultaneously multiply the viscosity ν by the same factor, to hold the Reynolds number constant. Thus this multiplicative velocity cascade could be purely formal and have nothing to do with the energy cascade. Let us check this physical idea.

First, we have to characterize the cascade. As remarked above [8,21], calling \bar{P} the distribution of $\ln|\delta v|$ we can write:

$$\bar{P}_r = G_{rr'} \otimes \bar{P}_{r'},$$

but also

$$\bar{P}_r = G_{rL} \otimes \bar{P}_L,$$

and

$$\bar{P}_{r'} = G_{r'L} \otimes \bar{P}_L,$$

where L is now a reference length (large scale) which we can take sufficiently large in order that the distribution does not evolve anymore. As these relations are assumed valid whatever \bar{P}_L , it implies:

$$G_{rL} = G_{rr'} \otimes G_{r'L}.$$

It is thus sufficient to characterize the distribution G_{rL} for any r . For this we can use its cumulants. From

$$\langle |\delta v|^p \rangle_r = \langle \alpha^p \rangle_{rL} \langle |\delta v|^p \rangle_L,$$

we can obtain experimentally

$$\langle \alpha^p \rangle_{rL} = \frac{\langle |\delta v|^p \rangle_r}{\langle |\delta v|^p \rangle_L}. \quad (14)$$

From now, we shall omit the index r or L for α :

$$\langle \alpha^p \rangle = \langle \exp(p \ln \alpha) \rangle = \exp \left\{ C_1 p + C_2 \frac{p^2}{2!} + \dots \right\}, \quad (15)$$

where C_i is the i th cumulant of G_{rL} . This gives the way to experimentally determine the coefficients C_i at each scale [20]. Plotting $(1/p) \ln \langle \alpha^p \rangle$ versus p , for p going from 1 to 6, gives a quasi-linear graph, which gives C_1 when linearly extrapolated to $p = 0$. Following the same procedure, the derivative of this graph gives C_2 , and the average slope of this derivative gives an estimate of C_3 . It is generally found [10,20] that C_3 is measurable but very small, while some closely related analysis [11] find $C_3 = 0$. In this paper we shall limit ourselves to the first two cumulants C_1 and C_2 , *i.e.* to the so-called log-normal approximation. $C_1 = \langle \ln \alpha \rangle$ is the average of $\ln \alpha$, and C_2 is the mean squared deviation:

$$C_2 = \langle (\ln \alpha - \langle \ln \alpha \rangle)^2 \rangle. \quad (16)$$

Figure 9 shows the behaviour of C_2 versus C_1 for different Reynolds numbers. They look as proportional down to very small scales. At the point marked by a bar, at small scales, the value of the logarithmic derivative of $\langle |\delta v|^3 \rangle$ is already:

$$\frac{d \ln \langle |\delta v|^3 \rangle}{d \ln r} = 2.5,$$

close to the dissipative range value: 3 (see insert). This proportionality on an extended range is equivalent to the Extended Self Similarity.

Now, the physical cascade picture has consequences on the behaviour of C_2 versus r . The cascade should stop and the signal should become smooth when the local Reynolds number crosses a critical value close to 1. A local Reynolds number can be estimated as $\alpha v_r/\nu$. Large α regions would become smooth for smaller scales than small α ones.

Above this dissipation threshold, in the inertial range, α roughly goes as $r^{1/3}$. Under the threshold, in the smooth dissipative range, α goes like r . This change of “velocity” $d \ln \alpha / d \ln r$ occurs first for small α , then for large ones, and thus stretches the distribution of $\ln \alpha$, increasing its width $\sqrt{C_2}$.

Thus the smoothing effect of the viscosity is completely different from that of low pass filtering the signal. In the latter case, the change of $d \ln \alpha / d \ln r$ occurs for all α at the same r . The distribution of α is not stretched and C_2 is not increased.

We can check this effect. We obtained a filtered $\{y_i\}$ file from the $\{x_i\}$ one (for $R_\lambda = 703$) through the exponential average:

$$y_i = \theta x_i + (1 - \theta) y_{i-1},$$

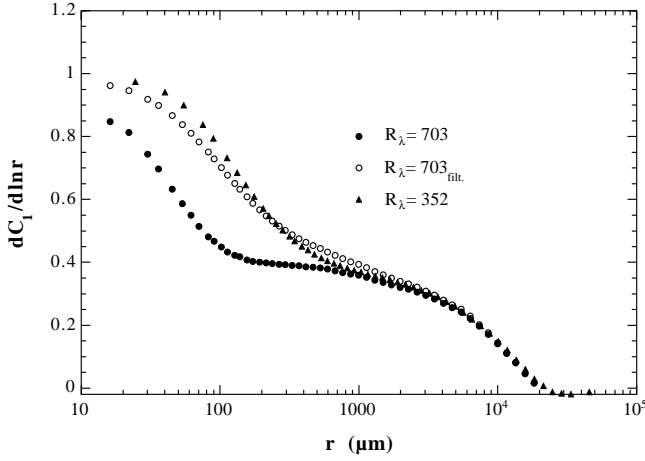


Fig. 10. Behaviour of $d \ln \langle \delta v^2 \rangle / d \ln r$ for the $R_\lambda = 703$ file and for the low pass filtered $R_\lambda = 703$ one, compared to the $R_\lambda = 352$ file. For $R_\lambda = 703$, the Kolmogorov scale is $\eta = 3.4 \mu\text{m}$ and the Taylor scale is $\lambda = 160 \mu\text{m}$. For $R_\lambda = 352$, $\eta = 9 \mu\text{m}$ and $\lambda = 320 \mu\text{m}$.

with $\theta = 0.1$. As the recording step roughly corresponds to the scale η , it is equivalent to averaging at the scale 10η .

As shown in Figure 10, the behaviour of $d \ln \langle \delta v^2 \rangle / d \ln r$ for the low pass filtered $R_\lambda = 703$ file, is very similar to the $R_\lambda = 352$ case. However the corresponding behaviours of $dC_2/d \ln r$ are completely different (Fig. 11a). The filtered file does not show the peak close to the dissipation scale, predicted (Fig. 11b) from the physical interpretation, and observed (Fig. 11a) on unfiltered files. This gives support to the physical origin of the cascade and to the physical significance and soundness of the quantity C_2 .

6 A model for C_2

Up to now, there is no model of intermittency which includes all the observed characteristics of the cascade:

- no cascade ($C_1 = C_2 = 0$) for r larger than some large scale, of the order of the integral one,
- approximate proportionality between C_1 and C_2 under this scale (E.S.S.) down to a dissipative scale,
- saturation of C_2 at the dissipative scale while C_1 becomes proportional to r .

Even an *ad hoc* model, however, would be useful for testing the compatibility of these apparently simultaneous properties. In this section, we try to construct such a model from the accepted physical ideas on the cascade.

As said above, local variations in the multiplier α can be seen as variation of the local mean squared deviation of the velocity difference $\sigma^2 = \alpha^2 v_0^2$. In the Langevin model these variations could in turn be attributed to local variations of ϵ but also of γ in such a way that v_0^2 remains constant. We cannot pretend to treat exactly this difficult

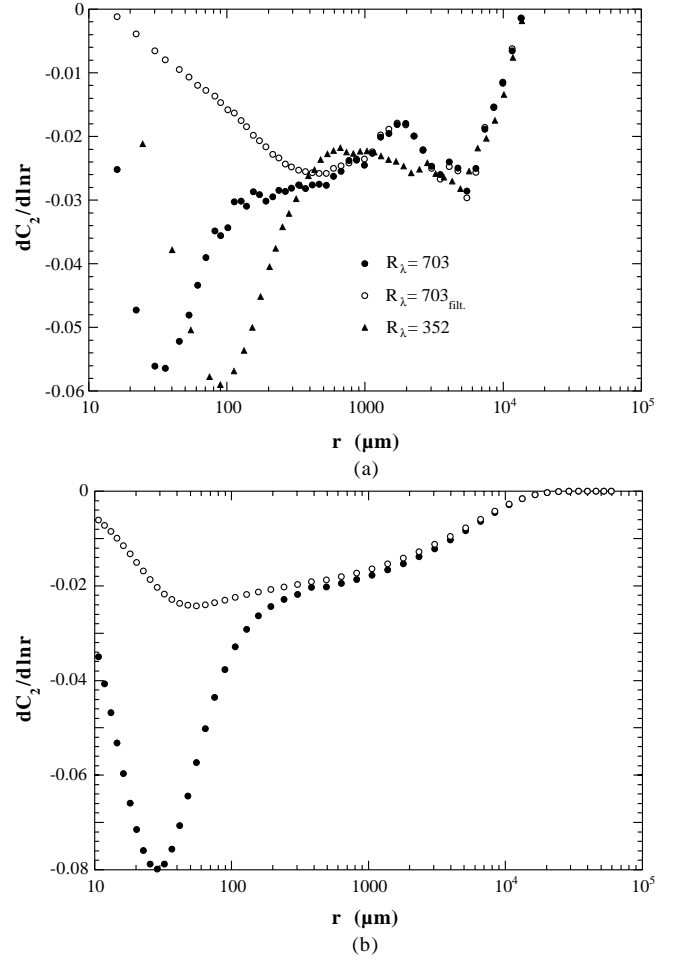


Fig. 11. (a) Behaviour of $dC_2/d \ln r$ (same files as in Fig. 10). (b) Model behaviour of $dC_2/d \ln r$ versus r : open symbols without stretching, full symbols with stretching.

problem, but we can modelize this effect *via* the ansatz:

$$\sigma^2 = \frac{r^2 v_0^2}{r^2 + \eta^2} E(y),$$

with $y = \epsilon \frac{t}{2v_0^2}$, and $E(y) = 1 - e^{-2y}$.

Then

$$\delta \ln \sigma = \left(\frac{\partial \ln \sigma}{\partial \ln \epsilon} \right)_{r,t} \delta \ln \epsilon = \frac{1}{2} \frac{d \ln E}{d \ln y} \delta \ln \epsilon,$$

and

$$\frac{dC_2}{d \ln r} = \frac{d}{d \ln r} \langle (\delta \ln \sigma)^2 \rangle = \left(\frac{1}{2} \frac{d \ln E}{d \ln y} \right)^2 \frac{d}{d \ln r} \langle (\delta \ln \epsilon)^2 \rangle.$$

This is sufficient to understand why $C_1 = C_2 = 0$ at large scales. In this range E is independent of y , and both $dC_1/d \ln r$ and $dC_2/d \ln r$ are zero.

$d\langle(\delta \ln \epsilon)^2\rangle/d \ln r$ traduces the progression in scales of the energy cascade. Let us assimilate it with the progression of $\ln t$ in the Langevin model

$$\frac{d}{d \ln r} \langle(\delta \ln \epsilon)^2\rangle = K \frac{d \ln t}{d \ln r},$$

K being a constant. It is certainly true at very large Reynolds, in the inertial range, due to scale invariance, but not outside. We do not pretend to exactitude. We only make the simplest hypothesis. When the dissipative scales are reached, the cascade in ϵ is simply frozen, as the evolution of t is frozen *via* the Batchelor ansatz (Eq. (10)). For $r < \eta$, $d \ln t/d \ln r$ is zero and thus $dC_2/d \ln r$ is zero.

We can estimate $d \ln t/d \ln r$ *via*

$$\frac{dC_1}{d \ln r} \approx \frac{d \ln \sigma}{d \ln r} = \frac{1}{2} \frac{d \ln E}{d \ln y} \frac{d \ln t}{d \ln r} + \frac{\eta^2}{\eta^2 + r^2},$$

where we neglect the intermittency and thus the variation of ϵ compared to other terms. Then:

$$\frac{d \ln t}{d \ln r} = 2 \frac{d \ln y}{d \ln E} \left(\frac{dC_1}{d \ln r} - \frac{\eta^2}{\eta^2 + r^2} \right).$$

To eliminate all the quantities which are defined through a model, as $d \ln E/d \ln y$, we can remark that it can be approximated by $2dC_1/d \ln r$. Their ratio

$$\frac{d \ln t}{d \ln r} + 2 \frac{\eta^2}{\eta^2 + r^2} \frac{d \ln y}{d \ln E}$$

never vanishes, being 2 in the dissipative range, 2 in the large scales and 2/3 in the inertial scales. Thus, approximating $d \ln E/d \ln y$ by $2dC_1/d \ln r$ is equivalent to have a smoothly varying ‘‘constant’’ K . We finally thus propose:

$$\frac{dC_2}{d \ln r} = K \frac{dC_1}{d \ln r} \left(\frac{dC_1}{d \ln r} - \frac{\eta^2}{\eta^2 + r^2} \right).$$

Indeed, we do not have all the contributions to $dC_2/d \ln r$. The stretching effect we discussed in the previous section, due to variation in the drift ‘‘velocity’’ $dC_1/d \ln r$ of the distribution of $\ln \alpha$, is not taken into account. Before to show how we can make it, let us clarify the argument by some notation change: $x = \ln \alpha$, $z = \ln r$. The local Reynolds number:

$$Re_1 = \frac{\alpha v_0 r}{\nu},$$

is such that $\ln Re_1 = x + z + \text{cste}$.

Let us approximate the cumulative density function $c(x)$ by a linear function:

$$c(x) = D(x - \langle x \rangle) + \frac{1}{2},$$

or

$$x(c) = \langle x \rangle + \frac{1}{D} \left(c - \frac{1}{2} \right).$$

We then have for the average:

$$C_1 = \int_0^1 x dc = \langle x \rangle,$$

and for the mean squared deviation:

$$C_2 = \int_0^1 (x - \langle x \rangle)^2 dc = \frac{1}{12D^2}.$$

Differentiating the relation for $x(c)$ at constant c ($q = \partial \langle x \rangle / \partial z$):

$$\begin{aligned} \left(\frac{\partial x}{\partial z} \right)_c &= q - \frac{(c - \frac{1}{2})}{D^2} \frac{dD}{dz} \\ &= q + \frac{(x - \langle x \rangle)}{2} \frac{1}{C_2} \frac{dC_2}{dz} \end{aligned}$$

sum of a drift and of a widening of the distribution. The widening itself can be partly due to stretching, *i.e.* to a dependence of the drift with the variable x . To identify this term we can consider the second term as only taking into account the other sources of widening discussed previously, and take q as x dependent (indeed $x+z$ dependent as seen above):

$$q = q(\langle x \rangle + z) + (x - \langle x \rangle) \left(\frac{\partial q}{\partial x} \right)_z,$$

we then obtain:

$$\frac{dC_1}{dz} = \int_0^1 \frac{\partial x}{\partial z} dc = q(\langle x \rangle + z),$$

and

$$\frac{d^2 C_1}{dz^2} = \left(\frac{\partial q}{\partial x} \right)_z \left(\frac{dC_1}{dz} + 1 \right),$$

which gives:

$$\begin{aligned} \frac{dC_2}{dz} &= 2 \int_0^1 (x - \langle x \rangle) \frac{\partial x}{\partial z} dc \\ &= \left\{ 2 \left(\frac{\partial q}{\partial x} \right)_z + \frac{1}{C_2} \left(\frac{dC_2}{dz} \right)_{\text{other}} \right\} \int_0^1 (x - \langle x \rangle)^2 dc \\ &= 2 \frac{C_2}{1 + \frac{dC_1}{dz}} \frac{d^2 C_1}{dz^2} + \left(\frac{dC_2}{dz} \right)_{\text{other}}. \end{aligned}$$

All together we have the model equation for the evolution of C_2 , taking into account both the stretching and the cascade:

$$\begin{aligned} \frac{dC_2}{d \ln r} &= 2C_2 \frac{d^2 C_1}{d(\ln r)^2} \left(1 + \frac{dC_1}{d \ln r} \right)^{-1} \\ &\quad + K \frac{dC_1}{d \ln r} \left(\frac{dC_1}{d \ln r} - \frac{\eta^2}{\eta^2 + r^2} \right). \end{aligned}$$

Note that, dividing by K , all adjustable parameters disappear for the evolution of $Y = C_2/K$:

$$\begin{aligned} \frac{dY}{d \ln r} &= 2Y \frac{d^2 C_1}{d(\ln r)^2} \left(1 + \frac{dC_1}{d \ln r} \right)^{-1} \\ &\quad + \frac{dC_1}{d \ln r} \left(\frac{dC_1}{d \ln r} - \frac{\eta^2}{\eta^2 + r^2} \right). \end{aligned}$$

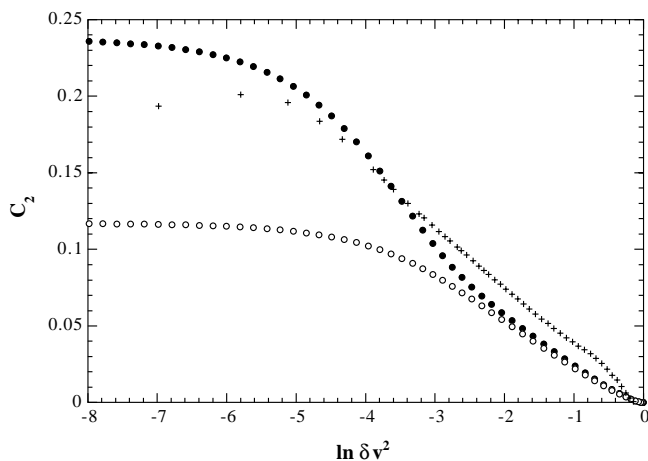


Fig. 12. Model evolution of C_2 versus $\ln \delta v^2$. Open symbols: without stretching, full symbols: with stretching. For comparison, experimental points for $R_\lambda = 703$ are also plotted with crosses.

We can also remark that, for large Reynolds numbers, in the inertial range $dC_1/d\ln r \approx 1/3$ and $d^2C_1/d(\ln r)^2 \approx 0$ which gives $dC_2/d\ln r \approx K/9$. Thus K is close to the parameter μ of the Kolmogorov-Obukov theory $K \approx \mu \approx 0.2$.

7 Discussion and conclusion

The model evolution for intermittency we derived above shows no indication of Extended Self Similarity. $dC_2/d\ln r$ is never proportional to $dC_1/d\ln r$, except in the trivial case where they both are constant, in the inertial range of very large Reynolds numbers. Nevertheless, the evolution we can infer from it, as shown in Figure 12, is close to the experimental one.

Independently of what occurs in real life, we can see for the model that this apparent linear dependence of C_2 versus C_1 is an artefact. This was already suggested, on other grounds, by previous authors [26]. At large scale, the part where $dC_1/d\ln r$ goes to zero poorly contributes to the evolution of C_1 and C_2 . Most of the variations can be attributed to the plateau where both derivatives $dC_i/d\ln r$ are nearly constant. On the other side the stretching of the distribution gives a rise in $dC_2/d\ln r$, which mimics the related rise in $dC_1/d\ln r$. Considering only the stretching gives:

$$\frac{1}{C_2} \frac{dC_2}{d\ln r} = 2 \frac{d^2C_1}{d(\ln r)^2} \left(1 + \frac{dC_1}{d\ln r} \right)^{-1},$$

and

$$C_2 = A \left(1 + \frac{dC_1}{d\ln r} \right)^2,$$

where A is some constant. Thus C_2 raises from a factor larger than 2 ($\approx 9/4$) at the dissipative range which strongly enhances the apparent range of proportionality

between C_1 and C_2 . However, this change occurs on a range proportional to $\sqrt{C_2}$, giving a slope which raises when the Reynolds number increases, as

$$\sqrt{C_2} \propto \sqrt{\ln Re}.$$

Thus E.S.S. remains questionable and, with it, the procedure for improving the scaling exponent determination. But the evidence of the stretching effect gives a strong support to the physical picture which is behind the cascade models. On the other hand, despite the spectacular effects of intermittency on the wings of the velocity differences pdf, it could be treated as a simple correction. The main physics is that of largely independent increments for the velocity differences. The real origin of these increments, which could be the large scale pressure differences, has to be elucidated.

References

1. A.S. Monin, A.M. Yaglom, *Statistical fluid mechanics* (M.I.T. Press, Cambridge, 1975), Vols. 1 & 2.
2. R. Cont, J.-P. Bouchaud, *Eur. Phys. J. B* **6**, 543 (1998).
3. S. Ghashghaie, W. Breyman, J. Peinke, P. Talkner, Y. Dodge, *Nature* **381**, 767 (1996).
4. A. Turiel, G. Mato, N. Parga, J.-P. Nadal, *Phys. Rev. Lett.* **80**, 1098 (1998).
5. U. Frisch, *Turbulence, the legacy of A.N. Kolmogorov* (Univ. Press, Cambridge, 1995).
6. M. Nelkin, *Adv. Phys. (UK)* **43**, 143 (1994).
7. B. Castaing, Y. Gagne, E. Hopfinger, *Physica D* **46**, 177 (1990).
8. B. Castaing, *J. Phys. II France* **6**, 105 (1996); B. Castaing, Y. Gagne, in *Turbulence in spatially extended systems*, edited by R. Benzi, C. Basdevant, S. Ciliberto (Les Houches, 1993).
9. B. Chabaud, A. Naert, J. Peinke, F. Chillà, B. Castaing, B. Hébral, *Phys. Rev. Lett.* **73**, 3227 (1994).
10. H. Kahalerras, Ph.D. thesis, University of Grenoble I, 1997.
11. A. Arneodo, S. Manneville, J.-F. Muzy, *Eur. Phys. J. B* **1**, 129 (1998).
12. R. Benzi, S. Ciliberto, R. Tripicione, C. Baudet, F. Massaioli, S. Succi, *Phys. Rev. E* **48**, R29 (1993).
13. O. Chanal, Ph.D. thesis, Institut National Polytechnique, Grenoble, 1998.
14. O. Chanal, B. Baguenard, O. Béthoux, B. Chabaud, *Rev. Sci. Instrum.* **68**, 2442 (1997).
15. F. Anselmet, Y. Gagne, E.J. Hopfinger, R.A. Antonia, *J. Fluid Mech.* **140**, 63 (1984).
16. V. Emsellem, *C. R. Acad. Sci. (Paris)* **322**, 11 (1996).
17. J.-F. Pinton, R. Labbé, *J. Phys. II France* **4**, 1461 (1994).
18. J. Lumley, *Phys. Fluids* **8**, 1056 (1965).
19. Y. Malécot, Ph.D. thesis, University of Grenoble I, 1998.
20. A. Naert, B. Chabaud, B. Hébral, B. Castaing, in *Advances in Turbulence*, edited by S. Gavrilakis *et al.* (Kluwer Academic Publ., 1996), Vol. VI.
21. E. Linberg, *Phys. Fluids* **11**, 510 (1999).
22. F. Moisy, P. Tabeling, H. Willaime, *Phys. Rev. Lett.* **82**, 3994 (1999).
23. J. Qian, *Phys. Rev. E* **60**, 3409 (1999).
24. Z.S. She, *Fluid Dyn. Res.* **8**, 143 (1991).
25. L.F. Richardson, *Proc. Roy. Soc. A* **97**, 354 (1922).
26. C. Meneveau, *Phys. Rev. E* **54**, 3657 (1996).